

Chiral Phonon activated Spin Seebeck Effect

Xiao Li,¹ Jinluo Cheng,² Lifa Zhang,^{1,*} and Jun Zhou^{1,†}

¹*NNU-SULI Thermal Energy Research Center (NSTER) and Center for Quantum Transport and Thermal Energy Science (CQTES),*

School of Physics and Technology, Nanjing Normal University, Nanjing 210023, China

²*Changchun Institute of Optics, Fine Mechanics and Physics, Chinese Academy of Science, Changchun 130033, China*

(Dated: May 19, 2021)

Efficient generation of spin polarization is very important for spintronics and quantum computation. We propose a new mechanism of Chiral Phonon activated Spin Seebeck (CPASS) effect in nonmagnetic materials in the absence of magnetic field and spin-orbital coupling. Owing to nonequilibrium distribution of chiral phonons under temperature gradient, we investigate the resulted chiral phonon activated spin polarization by solving the Boltzmann transport equation. The CPASS coefficients, with both band and phonon-drag contributions, exhibit linear dependence on the temperature gradient. The above two contributions are opposite for negative charge carriers and their relative magnitude is tunable by the chemical potential modulation. The CPASS effect where the spin accumulation is induced by chiral phonons, provides opportunities for the exploration of advanced spintronic devices based on chiral materials even in the absence of magnetic order and spin-orbit coupling.

Introduction.— The magnetism induced by phonons in solids has been ignored for a long time since phonons were traditionally regarded as linearly polarized and had no angular momentum. This circumstance has been changed since the discovery of nonzero angular momentum in chiral materials [1–5]. The "vibrational angular momentum" of chiral phonon, which describes the coupled-vibration-rotation of ions, was found to be important in nonequilibrium state when a temperature gradient is applied as an example [6]. The net magnetic moment induced by chiral phonons was firstly thought to be much smaller than the Bohr magneton [3, 6]. Lately, unexpected large magnetic moment was found in experiment [7]. It was possibly attributed the phonon-modified electronic energy together with the momentum-space Berry curvature [8].

We recognize that such large magnetic moment can be used to generate spin-polarized electrons which plays a crucial rule in the field of spintronics [9]. Usually, magnetism and/or spin-orbit interaction are indispensable to the manipulation the electron spin. People found that the chirality of materials, which characterizes the spatial inversion symmetry, provides an alternative source of spin polarization [10]. As early as 1995, Mayer and Kessler [11] measured the spin-dependent attenuation of electron beams through a vapor of chiral molecules due to the spin-orbit coupling. However, the measured signal was found to be extremely low. In 2011, Göhler [12] reported a much stronger spin filter effect when electrons transport through double-stranded DNA. After that, the widely observed spin polarization in various chiral materials led to the rise of a field called the chiral-induced spin selectivity (CISS) effect [13, 14]. The mechanism of CISS is still unclear because there is no magnetic field and the spin-orbit coupling in organic molecules is very low due

to the absence of heavy atoms. Different origins of CISS were proposed, for example, the electric field pumping effect [15], the electron transmission through helical potential [16, 17], the interplay of spin-orbit coupling and dipolar potential [18]. We believe that the CISS effect could be induced by chiral phonon because the electron spin is coupled to the phonon angular momentum in a similar way to the spin-rotation coupling [19, 20].

It is well known that the temperature gradient is able to generate spin voltage in magnets and materials with spin-orbit coupling. Such effect is called the spin Seebeck effect [21, 22]. Is it possible to utilize the temperature gradient to generate spin voltage in chiral materials in the absence of magnet and spin-orbit coupling?

In this Letter, we theoretically investigate the chiral phonon activated spin Seebeck (CPASS) effect due to nonequilibrium distribution of chiral phonons under temperature gradient in chiral materials, by the Boltzmann transport equation. The temperature gradient does not only lift the spin degeneracy but also play as the driving force of spin accumulation or spin current as shown in Fig. 1. As a result, a net spin accumulation is created, with both the phonon-drag and band transport contributions. The CPASS coefficients linearly depend on temperature gradient and the spin accumulation is found to be nearly quadratically increase with temperature gradient. The phonon-drag and band transport contribution are opposite with tunable relative magnitude by shifting the chemical potential. This new mechanism of the spin Seebeck effect proposed here gives full play to chiral phonons in spin-polarized transport, and provides another possible origin of CISS even in the absence of the magnetic field and strong spin-orbit coupling.

Theoretical formulation.— We begin with a net phonon angular momentum in chiral materials produced by non-

equilibrium distribution of chiral phonons under temperature gradient [6, 23], which exerts an effective magnetic field on Bloch electrons. Opposite Zeeman-type energy shifts are introduced in electronic band structure for opposite spins, with a magnitude of $\sigma\kappa\nabla T/2$. Here, the spin index, $\sigma = \pm 1$, denote opposite spins and ∇T is temperature gradient. κ is a material-specific strength coefficient of spin splitting and its sign depends on the chirality of the material. Assuming a parabolic dispersion, the electronic band energy reads,

$$\epsilon_\sigma(\mathbf{k}) = \hbar^2 k^2 / 2m + \sigma\kappa\nabla T / 2, \quad (1)$$

where m is the electron effective mass, and \mathbf{k} denote the wave vector of Bloch electron, which, together with σ , labels the electronic state. It is noted that the spin splitting here is not contributed from the spin-orbit coupling and applies to a chiral material composed of light elements as well.

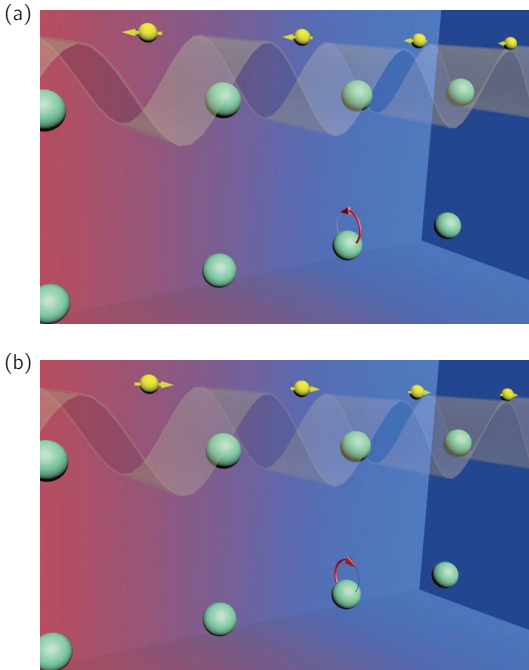


FIG. 1: Schematic depiction of the CPASS effect in chiral materials. (a) and (b) correspond to chiral phonons with opposite circular motions of the nuclei, giving rise to opposite spin polarization of electrons, respectively. The blue and yellow balls stand for the nuclei and electrons, respectively. The red arcs represent atomic circular motions with arrows denoting directions of the motions. The arrows on electrons point to the spin directions. A red-to-blue gradient background stands for an applied temperature gradient, and the wave for the heat current.

Given the above spin splitting, we investigate spin-dependent transport behavior under temperature gradi-

ent using the Boltzmann equation, which is given as

$$\begin{aligned} \mathbf{v}_\sigma(\mathbf{k}) \cdot \left\{ \nabla \mu_\sigma + [\epsilon_\sigma(\mathbf{k}) - \mu_\sigma] \frac{\nabla T}{T} \right\} \left[-\frac{\partial f_\sigma^0(\mathbf{k})}{\partial \epsilon_\sigma(\mathbf{k})} \right] \\ = -\frac{\partial f_\sigma(\mathbf{k})}{\tau_\sigma^e(\mathbf{k})} - \frac{\partial f_\sigma(\mathbf{k})}{\partial t} \Big|_{pd} \end{aligned} \quad (2)$$

The left-hand side (LHS) and right-hand side (RHS) of the equation correspond to the drift terms and collision integrals, respectively. $f_\sigma(\mathbf{k})$ and $\mathbf{v}_\sigma(\mathbf{k})$ are the electron's distribution function and group velocity, respectively. $f_\sigma(\mathbf{k}) = f_\sigma^0(\mathbf{k}) + \delta f_\sigma(\mathbf{k})$, where the equilibrium distribution function, $f_\sigma^0(\mathbf{k}) = [e^{\frac{\epsilon_\sigma(\mathbf{k}) - \mu_\sigma}{k_B T}} + 1]^{-1}$ and $\delta f_\sigma(\mathbf{k})$ is the derivation from the equilibrium. μ_σ is chemical potential and T is the temperature, while $\nabla \mu_\sigma$ and ∇T are corresponding spatial gradients. The collision integrals in RHS take into account multiple scattering processes, i.e. electron-phonon and impurity scatterings, with $\tau_\sigma^e(\mathbf{k})$ being a total electron relaxation time. The electron-phonon scattering contributes an phonon-drag electrical current, $\frac{\partial f_\sigma(\mathbf{k})}{\partial t} \Big|_{pd}$, which is written as,

$$\begin{aligned} \frac{\partial f_\sigma(\mathbf{k})}{\partial t} \Big|_{pd} = & \frac{2\pi}{\hbar} \sum_{\lambda} \int \frac{d^3 q}{(2\pi)^3} |M_\lambda(\mathbf{q})|^2 \{ [f_\sigma^0(\mathbf{k}) - f_\sigma^0(\mathbf{k} + \mathbf{q})] \delta_1 \\ & + [f_\sigma^0(\mathbf{k}) - f_\sigma^0(\mathbf{k} - \mathbf{q})] \delta_2 \} \delta n_\lambda(\mathbf{q}) \end{aligned} \quad (3)$$

In the phonon-drag term, \mathbf{q} and λ are the phonon's wave vector and band index, respectively. $|M_\lambda(\mathbf{q})|^2$ is the scattering matrix element. $\delta n_\lambda(\mathbf{q})$ is the derivation from the phonon distribution function $n_\lambda^0(\mathbf{q}) = [e^{\frac{\hbar\omega_\lambda(\mathbf{q})}{k_B T}} - 1]^{-1}$, where $\omega_\lambda(\mathbf{q})$ is the phonon eigenfrequency. According to the phonon Boltzmann equation, $\delta n_\lambda(\mathbf{q})$ is computed as $-\tau_\lambda(\mathbf{q}) \frac{\mathbf{v}_\lambda(\mathbf{q}) \cdot \nabla T}{k_B T^2} \hbar \omega_\lambda(\mathbf{q}) n_\lambda^0(\mathbf{q}) [n_\lambda^0(\mathbf{q}) + 1]$, with $\tau_\lambda(\mathbf{q})$ and $\mathbf{v}_\lambda(\mathbf{q})$ being the phonon's relaxation time and velocity, respectively. According to the momentum conservation in the electron-phonon scattering, a phonon with a given \mathbf{q} enables the scatterings between electronic states \mathbf{k} and $\mathbf{k}' = \mathbf{k} \pm \mathbf{q}$. The energy conservation is embodied in two Dirac delta functions, $\delta_1 = \delta[\epsilon_\sigma(\mathbf{k}) - \epsilon_\sigma(\mathbf{k} + \mathbf{q}) + \hbar\omega_\lambda(\mathbf{q})]$ and $\delta_2 = \delta[\epsilon_\sigma(\mathbf{k}) - \epsilon_\sigma(\mathbf{k} - \mathbf{q}) - \hbar\omega_\lambda(\mathbf{q})]$.

A open circuit condition in the CPASS effect corresponds to $\int \frac{d^3 k}{(2\pi)^3} \mathbf{v}_\sigma(\mathbf{k}) \delta f_\sigma(\mathbf{k}) = 0$, that is, there is no electron flow. Considering that $\delta f_\sigma(\mathbf{k})$ can be expressed by the drift and the phonon-drag terms according to Eq. (2) and assuming all vectors are parallel (e.g. along x -axis hereafter) for simplicity, the above condition is rewritten as

$$L_\sigma^{pd} \nabla T + L_\sigma^b \nabla T + L_\sigma \nabla \mu_\sigma = 0 \quad (4)$$

with

$$L_\sigma^{pd} = \frac{1}{\nabla T} \int \frac{d^3 k}{(2\pi)^3} v_{\sigma,x}(\mathbf{k}) \tau_\sigma^e(\mathbf{k}) \frac{\partial f_\sigma(\mathbf{k})}{\partial t} \Big|_{pd} \quad (5a)$$

$$L_\sigma^b = \frac{1}{T} \int \frac{d^3k}{(2\pi)^3} v_{\sigma,x}^2(\mathbf{k}) \tau_\sigma^e(\mathbf{k}) [\epsilon_\sigma(\mathbf{k}) - \mu_\sigma] \left[-\frac{\partial f_\sigma^0(\mathbf{k})}{\partial \epsilon_\sigma(\mathbf{k})} \right] \quad (5b)$$

$$L_\sigma = \int \frac{d^3k}{(2\pi)^3} v_{\sigma,x}^2(\mathbf{k}) \tau_\sigma^e(\mathbf{k}) \left[-\frac{\partial f_\sigma^0(\mathbf{k})}{\partial \epsilon_\sigma(\mathbf{k})} \right] \quad (5c)$$

where the integrals L_σ^{pd} and L_σ^b are explicitly associated with the phonon-drag effect and electronic band transport, respectively, while L_σ is a longitudinal conductivity of a unit charge. The explicit ∇T in the first term of LHS of Eq. (4) is extracted from $\delta n_\lambda(\mathbf{q})$ in $\frac{\partial f_\sigma(\mathbf{k})}{\partial t}|_{pd}$.

Taking into account opposite spins in Eq. (4), the chiral-phonon-induced spin accumulation generated in non-magnetic chiral materials can be obtained as

$$\nabla \delta \mu = \nabla (\mu_+ - \mu_-) = - \left(\frac{L_+^{pd}}{L_+} - \frac{L_-^{pd}}{L_-} \right) \nabla T - \left(\frac{L_+^b}{L_+} - \frac{L_-^b}{L_-} \right) \nabla T \quad (6)$$

Two terms of RHS of Eq. 6 correspond to the contributions from the phonon-drag effect and the electronic band transport, respectively. The total CPASS coefficient is further given as, $S_{tot} = \nabla \delta \mu / \nabla T$, with two corresponding contributions denoted by S_{pd} and S_b , where e represents the electron's charge. More details on the formula derivation of the chiral-phonon-induced spin Seebeck effect can be found in Supplemental Information (S.I. hereafter).

For the above CPASS effect, it is noted phonon modes are involved in two processes, i.e. inducing spin splitting in the band structure and phonon-drag current. The related phonon modes involved in the two processes are not necessary to be the same. For the phonon-drag current described by Eq. (3), longitudinal acoustic (LA) phonon is regard as a major contributor, since the LA phonon has a larger non-equilibrium population, $\delta n_\lambda(\mathbf{q})$, associated with its larger equilibrium phonon distribution $n_\lambda^0(\mathbf{q})$ and larger group velocity $v_\lambda(\mathbf{q})$ compared with optical branches. In contrast, chiral phonons with nonzero angular momentum, inducing the the spin splitting, are considered to exist in the entire phonon Brillouin zone except for the high-symmetry \mathbf{q} points, e.g. the Brillouin zone center with the time-reversal symmetry [6], and each phonon mode's contribution depends on not only its non-equilibrium population but also the magnitude of its angular momentum. Therefore, we take into account only LA modes in the following calculation of the phonon-drag current for simplicity, while the contributions from all chiral phonons are embodied in the parameter κ that determines the magnitude of spin splitting.

In the numerical calculation, for the LA phonon involved in the electron-phonon scattering, the phonon dispersion is approximately linear in the neighborhood of phonon Brillouin zone center, i.e. $\omega_{LA}(\mathbf{q}) = c_{LA}q$, with a momentum-independent phonon velocity, c_{LA} . Taking into account the scattering of electron by LA phonons,

the scattering matrix element reads, $|M_\lambda(\mathbf{q})|^2 = \frac{D_a^2 \hbar q}{4\rho c_{LA}}$ with D_a and ρ being the deformation potential strength and mass density of the chiral material considered, respectively. By simplifying the delta function composed with quadratic terms in \mathbf{q}/\mathbf{k} in Eq. (3), setting the Debye wavenumber as the upper limit of the integration with respect to q , the spin accumulation in Eq. (6) is computed numerically. Calculation details and parameter choices are given in S.I., unless otherwise specified. The calculation results are demonstrated and discussed below.

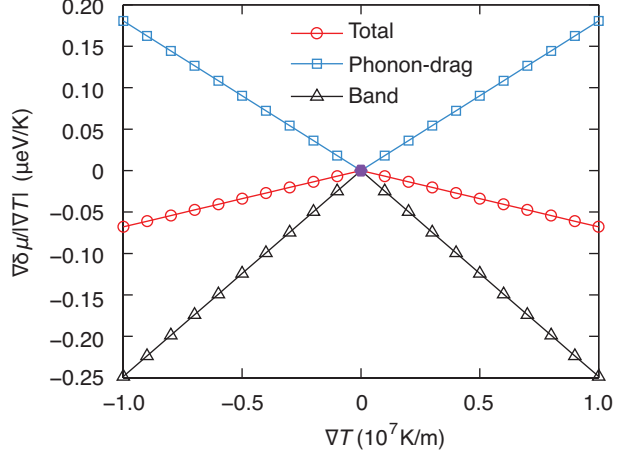


FIG. 2: Changes of CPASS coefficients with increasing temperature gradient. The phonon-drag and band contributions to the spin Seebeck effect are denoted by blue square and black triangle, respectively, while the total contribution is given by red circle. The parameters, $\mu = 0.2$ eV, $\kappa = 10^{-10}$ eV·m/K and $T = 300$ K.

Numerical results.—Figure 2 shows representative evolutions of the CPASS coefficients with the temperature gradient ∇T , where the band transport contribution S_b , phonon-drag contribution S_{pd} and their sum, i.e. total contribution S_{tot} are all plotted. The computed spin Seebeck coefficients are considerable using reasonable material-specific parameters, and they are expected to be measurable by readily experimental techniques. It is also found that the magnitudes of the coefficients increase linearly with increasing temperature gradient. That is, the spin accumulation, $\nabla \delta \mu$, has a quadratic dependency on temperature gradient. This is because besides the explicit ∇T in Eq. (6), ∇T is also included in $\epsilon_\sigma(\mathbf{k})$ with the spin splitting term from nonequilibrium phonon distribution under spatial temperature difference. In contrast, assuming that the spin splitting is independent on temperature gradient, the calculated spin Seebeck coefficients become constant with varied temperature gradient. The CPASS effect is thus more sensitive to temperature gradient. Besides, the band transport contribution and the phonon-drag contribution are always opposite in the parameter space considered when the carriers' charge is

regarded to be negative, and their relative magnitudes vary with parameter choices.

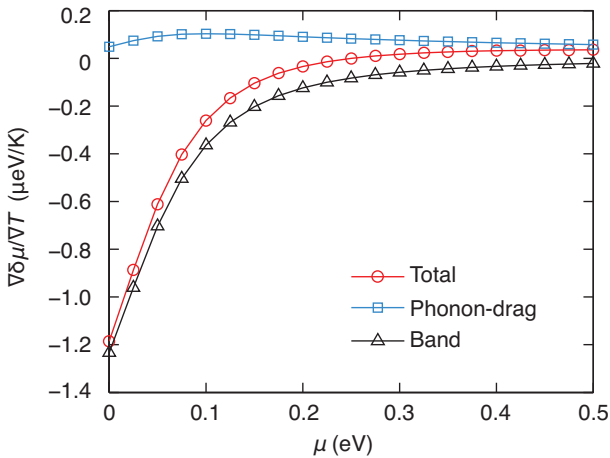


FIG. 3: Changes of CPASS coefficients with varied chemical potential. The parameters, $\nabla T = 5 \times 10^6$ K/m, $\kappa = 10^{-10}$ eV·m/K and $T = 300$ K.

Figure 3 demonstrate the changes of the CPASS coefficients at a given temperature gradient with the chemical potential, μ . When the chemical potential is set to the band edge ($\mu \approx 0$ eV), i.e. the system is in the non-degenerate limit, it is found that the band contribution to spin Seebeck coefficient is much larger than the phonon-drag contribution by several tens of times. As the chemical potential is shifted upwards, the band contribution is always decreased, by up to more than one order of magnitude, while the phonon-drag contribution is varied within the same order. As a result, the band contribution become closer to and then smaller than the phonon-drag contribution in magnitude. Given that the two contributions are opposite, a switch of their relative magnitudes leads to a sign change of the total CPASS coefficient. The μ -sensitive variation in the band contribution arises from the difference between the electronic band energy $\epsilon_\sigma(\mathbf{k})$ and the chemical potential in Eq. (5b). When moving the chemical potential away from the band edge, the difference is not always positive for varied electronic energies, leading to the cancellation of the differences with opposite signs and consequent decreased band contribution to the CPASS effect.

The computed magnitudes of CPASS coefficients are further given as functions of the strength coefficient of the spin splitting, κ , embodied in the spin splitting term of Eq. 1, by a log-log scaled plot in Fig. 3, while the other parameters are kept unchanged. It is seen that the strengths of CPASS effect, including band and phonon-drag contributions, are all linearly proportional to κ and corresponding spin splitting in the band structure, over a large range of κ , according to the lines with the slope of 1 in the log-log plot. When $\kappa = 0$, i.e. the electronic band has no spin splitting, the computed CPASS coef-

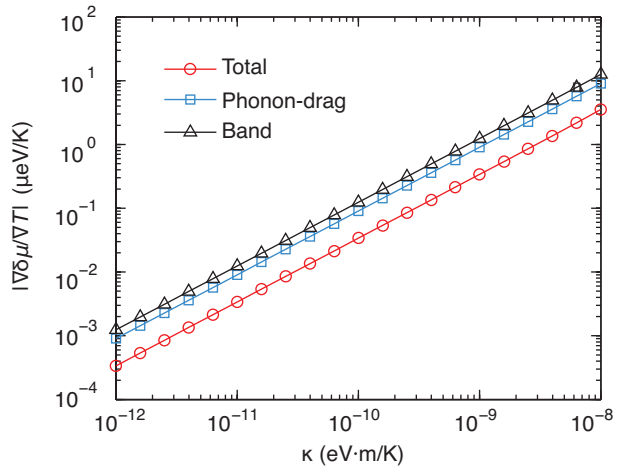


FIG. 4: Changes in magnitudes of CPASS coefficients with varied strength coefficient of the spin splitting. Both axes are plotted using a logarithmic scale. The parameters, $\mu = 0.2$ eV, $\nabla T = 5 \times 10^6$ K/m and $T = 300$ K.

ficients are vanishing as well. Therefore, the spin splitting induced by the nonequilibrium distribution of chiral phonons under temperature gradient is necessary for the CPASS in chiral materials. We pointed out that, when the sign of κ is changed, the calculated spin accumulation must reverse because the last term in Eq. (1) is unchanged when $\sigma \rightarrow -\sigma$ and $\kappa \rightarrow -\kappa$. Therefore, the left-handed and right-handed materials lead to opposite spin polarizations.

Summary.— The above study on the CPASS effect provides a promising explanation on the CISS observed in chiral materials where both magnetic order and strong spin-orbit coupling are absent. Furthermore, the spin Seebeck effect proposed here is not limited to chiral materials and it is expected to have generalizations to other non-centrosymmetric materials, including polar materials, since these materials can also obtain net phonon angular momentum and effective magnetic field under temperature gradient [6]. While our highly symmetry model has only nonvanishing longitudinal spin Seebeck coefficient, distinct spin Seebeck response tensors, including longitudinal and transverse components, are expected in various non-centrosymmetric materials with different crystalline symmetries. It is worth quantitative calculations on the response tensor of more realistic materials by e.g. first-principles methods to provide more material candidates for the CPASS effect.

Very recently, our colleagues have observed such CPASS effect by ultrafast pump-probe experiment in organic-inorganic hybrid perovskites [24]. The CPASS effect provides opportunities for the exploration of advanced spintronic devices based on chiral materials even in the absence of magnetic order and spin-orbit coupling.

ACKNOWLEDGMENTS

We acknowledge support from the National Natural Science Foundation of China (No. 11904173, No. 11890703). X.L. is also supported by the Jiangsu Specially-Appointed Professor Program.

* Electronic address: phyzlf@njnu.edu.cn

† Electronic address: zhoujunzhou@njnu.edu.cn

- [1] L. Zhang and Q. Niu, Phys. Rev. Lett. **112**, 085503 (2014).
- [2] L. Zhang and Q. Niu, Phys. Rev. Lett. **115**, 115502 (2015).
- [3] D. M. Juraschek and N. A. Spaldin, Phys. Rev. Mater. **3**, 064405 (2019).
- [4] T. Nova, A. Cartella, A. Cantaluppi, M. Först, D. Bossini, R. Mikhaylovskiy, A. Kimel, R. Merlin, and A. Cavalleri, Nat. Phys. **13**, 132 (2017).
- [5] H. Zhu, J. Yi, M.-Y. Li, J. Xiao, L. Zhang, C.-W. Yang, R. A. Kaindl, L.-J. Li, Y. Wang, and X. Zhang, Science **359**, 579 (2018).
- [6] M. Hamada, E. Minamitani, M. Hirayama, and S. Murakami, Phys. Rev. Lett. **121**, 175301 (2018).
- [7] B. Cheng, T. Schumann, Y. Wang, X. Zhang, D. Barbalas, S. Stemmer, and N. P. Armitage, Nano Lett. **20**, 5991 (2020).
- [8] Y. Ren, C. Xiao, D. Saparov, and Q. Niu, arXiv **2103**, 05786 (2021).
- [9] D. Awschalom, D. Loss, and N. Samarth, *Semiconductor Spintronics and Quantum Computation* (Springer, New York, 2002).
- [10] G. L. Rikken, Science **331**, 864 (2011).
- [11] S. Mayer and J. Kessler, Phys. Rev. Lett. **74**, 4803 (1995).
- [12] B. Göhler, V. Hamelbeck, T. Z. Markus, M. Kettner, G. F. Hanne, Z. Vager, R. Naaman, and H. Zacharias, Science **331**, 894 (2011).
- [13] R. Naaman and D. H. Waldeck, Annu. Rev. Phys. Chem. **66**, 263 (2015).
- [14] K. Michaeli, V. Varade, R. Naaman, and D. H. Waldeck, J. Phys.: Condens. Matter **29**, 103002 (2017).
- [15] D. Rai and M. Galperin, J. Phys. Chem. C **117**, 13730 (2013).
- [16] A. A. Eremko and V. M. Loktev, Phys. Rev. B **88**, 165409 (2013).
- [17] R. Gutierrez, E. Díaz, R. Naaman, and G. Cuniberti, Phys. Rev. B **85**, 081404 (2012).
- [18] K. Michaeli and R. Naaman, J. Phys. Chem. C **123**, 17043 (2019).
- [19] M. Matsuo, J. Ieda, K. Harii, E. Saitoh, and S. Maekawa, Phys. Rev. B **87**, 180402 (2013).
- [20] M. Hamada, T. Yokoyama, and S. Murakami, Phys. Rev. B **92**, 060409 (2015).
- [21] K. Uchida, S. Takahashi, K. Harii, J. Ieda, W. Koshiba, K. Ando, S. Maekawa, and E. Saitoh, Nature **455**, 778 (2008).
- [22] H. Adachi, K. ichi Uchida, E. Saitoh, and S. Maekawa, Rep. Prog. Phys. **76**, 036501 (2013).
- [23] M. Hamada and S. Murakami, Phys. Rev. B **101**, 144306 (2020).
- [24] K. Kim, E. Vetter, Y. Liang, Y. Yang, X. Li, L. Zhang, J. Zhou, W. You, D. Sun, and J. Liu, to be submitted (2021).